

Utilizing COMSOL® in a workflow to assess stroke risks in a large set of patients carotid arteries

T. Probst¹, K. Richter¹, A. Hundertmark¹

1. Institute for Mathematics, Natural and Environmental Sciences, RPTU Kaiserslautern-Landau, Germany

Abstract

The bifurcation area of the carotid artery is of great importance in the medical risk assessment of strokes caused by pathological irregularities. Traditionally, physicians use the evaluation of stenosis degree, systolic and diastolic velocity measurements and individual characteristics like age, gender and more for valuation of stroke risks. Here, decision-making processes can be significantly improved with accurate flow field data obtained from simulations in patient-specific geometries. To create a large hemodynamic database of 110 individual artery morphologies we developed an automated workflow for numerical data generation utilizing the COMSOL Multiphysics® software.

Our automated workflow consists of 1. geometric preprocessing and simulation parameter setup, 2. simulation and 3. postprocessing and data export. Starting with preparations of simulation- and export-parameters, we use the centerline of each individual's vessel tree to determine morphology specific parameters for cutting the in- and outlets, analytically define areas around the bifurcation and the internal carotid area and also set up slicing planes in those areas to evaluate flow field variables. In addition, we calculate a special three-dimensional vector field on the vessel surface, which is integrated in COMSOL® to evaluate a directional wall shear stress parameter (WSS) in the postprocessing step. The carotid artery model is then imported with the CAD Import Module and is geometrically adapted in the geometry node of our COMSOL®-simulation template according to predefined parameters from step 1. In step 2. the blood flow is simulated by solving the incompressible Navier-Stokes equations for laminar flow. To ensure realistic flow volume distribution between the internal and external subbranches of the carotid vessel tree and thus to achieve a reliable simulation, we use resistance boundary conditions for each of the outlet surfaces. The workflow is completed with evaluation and export of computed and postprocessed data. Beside the flow variables like velocity and pressure we are particularly interested in the wall shear stresses (WSS) at the vessel surface. The created hemodynamic database of 110 patient cases has been successfully utilized to train a neural network for stenosis degree categorization based on the WSS and was integrated into an exploratory visualization tool for flow similarity analysis.

Keywords: CFD - hemodynamics – patient specific artery - centerline projection method - automated simulation workflow

Introduction

Cardiovascular diseases (CVDs) have a huge impact on modern society. They are, with an estimated death toll of 17.9 million in 2019, the leading cause for death globally [1]. Furthermore, they are extremely expensive e.g., they cost the United States about 240 billion dollars annually [2].

The most common form of CVD, atherosclerosis, results in inflammation of the inner wall of arteries due to endothelial stress and lipid metabolism, which leads to the narrowing of the artery and therefore to an insufficient supply of the brain with oxygen [3]. In this context the carotid artery, consisting of the carotid communis, which bifurcates into the interna and externa through the carotid bifurcation, whereby the former supply the brain with oxygen, is responsible for 18-25% of thromboembolic strokes and therefore enjoys special attention in the study of atherosclerosis [4]. Especially since atherosclerosis is no longer just a problem of western societies and old people but has developed into a complex global phenomenon that affects developing countries in particular and increasingly young people [5] [6]. Therefore, disease management and prevention tools

based on individual risk profiles are becoming increasingly important. Research into the numerical basis for modeling and simulation of the cardiovascular system and medical practice have been largely separated in the past. To combine both is the overreaching goal of our research project. To do this, 110 anonymized CTAs have been processed to 3D patient-specific geometries and centerlines of the carotid artery utilizing the *CarotidAnalyzer* tool [7]. Each of the resulting carotid artery data set available in [7] requires patient-specific simulation parameters that allow us to numerically analyze the patient's risk factors for atherosclerosis induced by blood flow exerted stresses and to obtain a data pool for further analysis or training a neural network. This new patient-oriented approach requires to process a large amount of data through (1) preprocessing, (2) simulation, and (3) postprocessing. Time becomes an important factor and so the aim of this paper is to present an efficient workflow of the above steps by utilizing COMSOL® and to support researchers and practitioners in the setup of their own practice with large sets of simulation cases as for instance patient specific arteries.

Simulation Setup

The simulation of blood flow in the patient-specific carotid artery is performed using single phase laminar flow model of COMSOL® Multiphysics based on incompressible Navier-Stokes equations,

$$\rho \frac{\partial \mathbf{u}}{\partial t} + \rho(\mathbf{u} \cdot \nabla)\mathbf{u} = \nabla \cdot (-p\mathbf{I} + 2\mu\mathbf{D}(\mathbf{u})) \quad (1)$$

$$\nabla \cdot \mathbf{u} = 0, \quad (2)$$

where the density was set to $\rho = 1060 \text{ kg/m}^3$ and the blood viscosity $\mu = 0.00345 \text{ Pa} \cdot \text{s}$. To limit the computational costs of creating the hemodynamic database, we assume rigid vessel walls and neglect their compliance, which would require to model the fluid-structure interaction. Therefore, we apply a no-slip boundary condition at the walls,

$$\mathbf{u} \equiv 0 \text{ on } \Gamma_{\text{wall}}.$$

To obtain a realistic flow behavior, pulsatile flow profile from Fig. 1 is applied using appropriate time-dependent velocity function prescribed at the inlet of the artery.

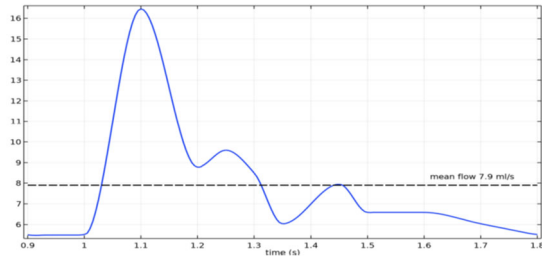


Figure 1: Pulsatile volumetric flowrate $Q_{in}(t)$ for one heartbeat, [22] [23].

To define realistic outflow boundary conditions, we assume that 70% of the blood flow arriving through the communis splits at the bifurcation into the interna and the remaining 30% flows through the externa-tree, regulated by intracranial artery system [8] [9]. To control this behavior and to waive the velocity definition at the outlets, which affects the flow patterns inside the volume of the carotid artery (CA) significantly, we adapted the resistance boundary condition principle arising from the coupling with lumped downstream model, see e.g., [10]. Here, the flow resistance is analogous to the electrical resistance and results as a ratio of pressure and volume flow, i.e.,

$$p = R \cdot Q. \quad (3)$$

The total resistance of the CA-tree is given by mean pressure and mean flow, $R_{\text{tot}} = \frac{p_{\text{mean}}}{Q_{\text{mean}}}$, where $p_{\text{mean}} = \frac{2}{3}p_{\text{dia}} + \frac{1}{3}p_{\text{sys}}$ is a combination of systolic and diastolic pressure and $Q_{\text{mean}} = \frac{1}{T} \int Q_{in}(t)dt$, is given by the inlet flowrate Q_{in} . Moreover, the 30% flow volume in the externa tree is divided in the ratio that the areas bear to each other. According to the Ohm's law for parallel circuits, for the total resistance of the arterial tree and the respective resistances of all branches it holds

$$R_{\text{tot}}^{-1} = R_{\text{int}}^{-1} + R_{\text{ext}}^{-1} = R_{\text{int}}^{-1} + R_{\text{ext}_1}^{-1} + \dots + R_{\text{ext}_n}^{-1}. \quad (4)$$

Finally, the resistance values to be applied for each outlet are obtained,

$$R_{\text{int}} = \frac{1}{0.7}R_{\text{tot}}, \quad R_{\text{ext}} = \frac{1}{0.3}R_{\text{tot}} \quad (5)$$

$$R_{\text{ext}_i} = \frac{\sum_j |\Gamma_{\text{ext}_j}|}{|\Gamma_{\text{ext}_i}|} R_{\text{ext}}. \quad (6)$$

In the resistance boundary condition, the pressure in the boundary stress is replaced according to Eq. (3), which is implemented in our simulation template by applying a *general stress* in the *boundary stress* node to the artery outlets $\Gamma_i = \Gamma_{\text{int}}, \Gamma_{\text{ext}_i}$. For that, the stress vector \mathbf{F} is replaced by

$$\mathbf{F} = \left(-R_i \cdot \int_{\Gamma_i} \mathbf{u} \cdot \mathbf{n} \, ds \right) \mathbf{n} + (2\mu\mathbf{D}(\mathbf{u}))\mathbf{n}, \quad (7)$$

applying the integral operators over outlet cross-sections to the normal velocity and using the components of the shear stress vector $(2\mu\mathbf{D}(\mathbf{u}))\mathbf{n}$ defined as variables $\text{Nbwwhw}\{\#\text{Nbwwhw}\} \{\#\text{Nbwwhw}\}$ in COMSOL®, see Fig. 2.

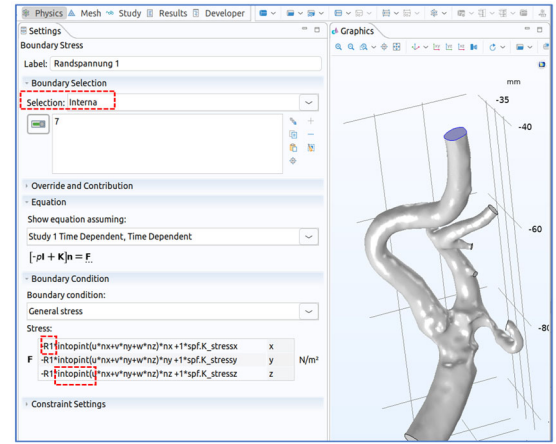


Figure 2: Implementing the resistance boundary condition (7) on interna branch outlet.

Risk factors: OSI & WSS

Cardiovascular risk descriptors as the wall shear stress (WSS), describing the endothelial stress exerted by blood forces on the wall tissue and its temporary change of direction described by oscillatory shear index (OSI) can be evaluated in postprocessing of the numerical data. The WSS vector ($\boldsymbol{\tau}_w$) is defined as a projection of the (Cauchy) stress vector $\mathbf{t}_f := -\mathbf{T}_f \mathbf{n} = (p\mathbf{I} - 2\mu\mathbf{D}(\mathbf{u}))\mathbf{n}$ into the tangential plane, i.e.,

$$\boldsymbol{\tau}_w = \mathbf{t}_f - \mathbf{t}_f \cdot \mathbf{n}, \quad (8)$$

where $\mathbf{t}_f \cdot \mathbf{n}$, denotes the normal component of the stress vector. WSS can be implemented using the variables for the components of stress vector \mathbf{t}_f , $\text{Wbwwhw}\{\#\text{Wbwwhw}\} \{\#\text{Wbwwhw}\}$ and of the normal vector \mathbf{n} , $\text{p hvk}\{\#\text{p hvk}\} \{\#\text{p hvk}\}$. Typically, a scalar value of WSS defined as its vector norm (or amplitude)

$$\tau_w^a = \|\boldsymbol{\tau}_w\|$$

is evaluated for cardiovascular risk indication by its high values, see e.g., [11]

Apart of high WSS values, also low, multi-directional and oscillating WSS is observed in sites with disturbed blood flow as helical or backflow, promoting the atherosclerotic processes, arterial lesions and plaque formations [12] [13]. To detect backflow, the flow multi-directionality and disturbances by a

surface indicator, we evaluate the longitudinal component of WSS-vector, associated with the artery main flow direction, see [14]

$$\tau_w^{\ell} = \tau_w \cdot \mathbf{t}_{\ell}, \quad (9)$$

where \mathbf{t}_{ℓ} is the tangential vector field aligned longitudinally along the vessel tree, constructed by centerline projection method in preprocessing as described below. The longitudinal WSS (9) can be evaluated within COMSOL® as follows,

```
0:siWbwzWw{-W [# #siWbwzWw]-W\##  
vsIWbwzWw}-W} #
```

where W [$\#W$ \ $\#W$] are components of a specially constructed tangential vector field.

The OSI is derived from wall shear stress by the normalization of the temporal mean over one cardiovascular cycle,

$$OSI = \frac{1}{2} \left(1 - \frac{\| \int \tau_w dt \|}{\int \|\tau_w\| dt} \right). \quad (10)$$

The values of OSI (10) lay in the range between 0 and $\frac{1}{2}$ and its highest value describes high temporal and directional change of WSS, having injurious character on the vessel tissue [12] [15] [16] [17]. However, its lowest value covers persistent positive as well as negative WSS values, thus the local persistent oppose flow cannot be detected by (10). In addition, longitudinal OSI based on the scalar valued longitudinal WSS,

$$OSI^{\ell} = \frac{1}{2} \left(1 - \frac{\int \tau_w^{\ell} dt}{\int |\tau_w^{\ell}| dt} \right) \quad (11)$$

is evaluated in our study, spanning the interval of values between 0 and 1, where $\frac{1}{2}$ accounts for highest directional oscillations of τ_w^{ℓ} similarly as in definition (10), and its maximal value 1 describes sites with persistent oppose or side flow, thus vortices or flow disturbances as helical flow, see also the discussion on directional risk measures in [14].

Workflow

To preprocess (1), simulate (2) and postprocess (3) simulations efficiently through the 110 individual carotid arteries, we set up an automated workflow to speed up the work routine with COMSOL® Multiphysics, see Fig. 3. Most of the preprocessing steps are done outside COMSOL®. For this purpose we develop *Octave* [18] scripts, which compute geometric parameters and generate further simulation inputs or definitions based on individual patient geometry and its centerline, utilizing additionally *Blender* [19] for more precise visualization of artery surface and centerline. The parameters for the cropping of the 3D artery to a CFD computational domain and geometric setting for exporting two-dimensional data (slices or surface data) of specific CA sites are defined in the preprocessing steps. Moreover, longitudinal surface tangent vectors \mathbf{t}_{ℓ} for evaluation of longitudinal WSS (9) are pre-computed and expressions or integral operators for resistance boundary conditions, see Fig. 2 and Eqs. (5-7) are generated. Our COMSOL® simulation template is set up by importing these individually prepared, morphology specific

parameters, variables and definitions into COMSOL® to define the physical problem and boundary conditions. After further adapting of the simulation template to the individual case, simulations can be run from a queue of several prepared simulation files and in parallel. Note, that geometric preprocessing is of high importance in our workflow, where non consistent parameters lead to time intensive corrections in the individual simulation file itself or to long computational times. In the simulation postprocessing, specific flow volume or surface data and derived risk descriptors as WSS, OSI, (8)-(11), are evaluated. These are pre-defined in the export node of the simulation template. For the schematic overview of the simulation workflow see Fig. 3., more detailed description of the individual workflow steps follows.

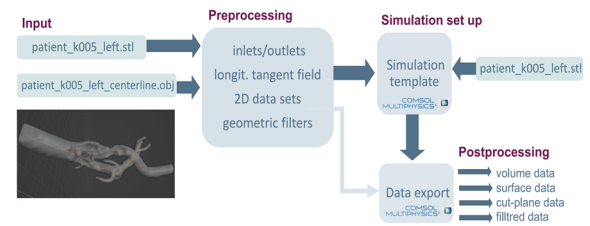


Figure 3: Schematic overview of the workflow.

Preprocessing: parameters, variables & tangential field preparation

In the preprocessing, we utilize *Octave* [18] to prepare simulations in an CA-tree up to a maximum of 7 outlets. As input our program needs the geometry as STL file in ASCII format and the centerline as OBJ file.

Since there are no inlets and outlets defined in the original segmented geometrical objects, the geometry must be cropped using cut-planes. The cutting planes are defined orthogonal to the course of the

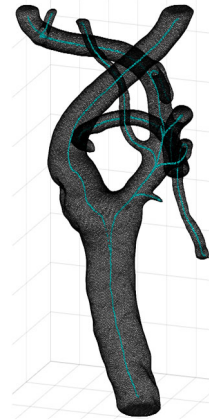


Figure 4: Visualization of geometry and centerline

centerline, i.e., the centerline tangential vectors at the in- and outlets define the normal vectors of the cutting planes, where the corresponding points of the centerline are selected manually.

Since the resistances defined in eq. (6), applied in stress expressions, cp. (7), depend on the number of externa outlets, a respective number of outlets must be entered as well. To evaluate and export the volume quantities (velocity, vorticity, pressure) in reduced two-dimensional representation of *slice plots*, planes parallel to the course of the artery in the areas of interest as the initial interna branch and the bifurcation area must be defined. Here, two resp. three points for the interna and the bifurcation area are selected from the centerline by clicking in the *Octave* graphics window. From these, the centroid of the

collected points is calculated as the mean value of their x-, y- and z- coordinates. Then a singular value decomposition (SVD) is performed for the matrix which contains the connection vectors from the centroid to the selected points within the area of interest.

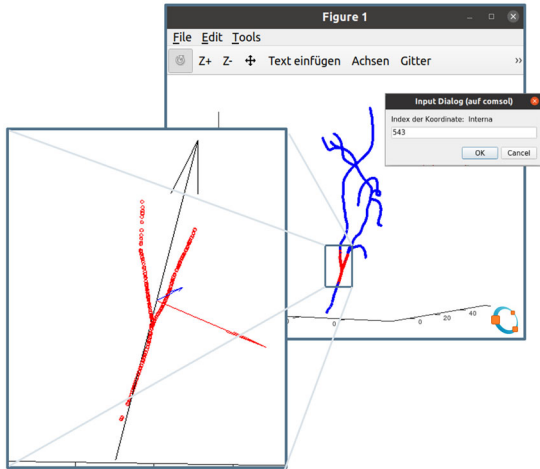


Figure 5: Selection of bifurcation area by entering its bounding points for SVD.

As result we get the normal vector \vec{n} and the two tangential vectors \vec{t} of the best fitting plane to the selected points. Finally, to use this plane to evaluate the volume field quantities, we apply the normal formula of the plane equation to derive three points on the plane that are used to define the *slice plots* in the *result* node. In evaluation of hemodynamic risk factors the surface of initial interna branch and of the bifurcation of CA are sites of interest as well. To define a logical expression that serves as a geometric filter for corresponding plots in our COMSOL®-template, the above-described centroid is considered as the center point $\mathbf{x}_0 = (x_0, y_0, z_0)$ of our filter-ellipsoid,

$$E(\mathbf{x}) = a(x - x_0)^p + b(y - y_0)^p + c(z - z_0)^p \leq R, \quad (12)$$

with $p = 2, 4, 6$ defining the concrete shape of the ellipsoid; the higher p , the more E becomes. The fixed values R , a , b and c are chosen appropriately for most cases, manual adjustments are needed only for few morphologies. In the above formulation (12) E has standard orientation, with main axes aligned with coordinate system and must be rotated to fit around the arterial branch (interna or bifurcation). In our settings the z-axis, i.e., the vector $\vec{s} = (0, 0, 1)^T$ must be rotated to one of the tangential vectors \vec{t} , obtained from the singular value decomposition above, that is closer to the main flow direction. The rotation is performed around the axis aligned with a vector $\vec{v} = (v_1, v_2, v_3) = \vec{t} \times \vec{s}$ and with rotation angle ϕ between \vec{s} and \vec{t} ,

$$\phi = \text{atan} \frac{|\vec{v}|}{|t_3|}, \quad (13)$$

where \vec{v} is the cross product of $\vec{t} = (t_1, t_2, t_3)$ and \vec{s} and orthogonal to both. Finally, the rotation matrix $\mathbf{R}_{\vec{v}}$ is a symmetric 3x3 matrix,

$$\mathbf{R}_{\vec{v}} = \begin{pmatrix} v_1^2 C + \cos \phi & v_1 v_2 C - v_3 \sin \phi & v_1 v_3 C + v_2 \sin \phi \\ v_2 v_1 C + \cos \phi & v_2^2 C + \cos \phi & v_2 v_3 C - v_1 \sin \phi \\ v_3 v_1 C - v_2 \sin \phi & v_3 v_2 C + v_1 \sin \phi & v_3^2 C + \cos \phi \end{pmatrix}$$

with $C = (1 - \cos \phi)$.

Applying $\mathbf{R}_{\vec{v}}$ to the spatial variables $\mathbf{x} = (x, y, z)$ in (12) gives the final geometric filter aligned with the course of artery. On Fig. 6 the application of such geometric filter to the surface data is presented.

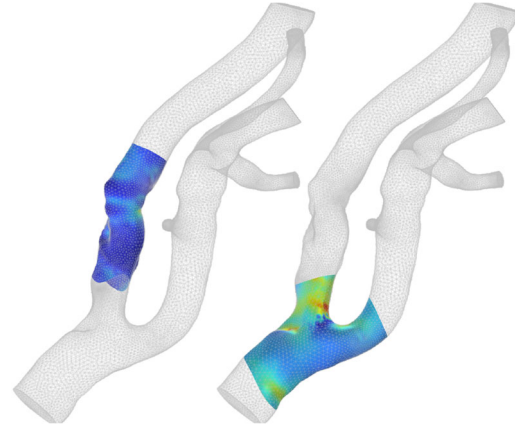


Figure 6: Final filter applied in COMSOL®.

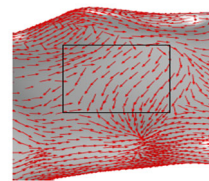


Figure 7: Generic COMSOL tangent field, [14].

To evaluate the longitudinal WSS (9) and OSI (11), a tangential surface vectors \vec{t}_p aligned with the main flow direction, are needed. The automatically generated tangent vectors from COMSOL® do not follow the overall course of the artery on complex geometry surfaces, see Fig. 7. This applies especially in areas of craggy surfaces of plaque depositions, where the focus of our analysis lies. Therefore, in a last step of the preprocessing, a proper longitudinal tangential field on the surface of the artery is constructed. Here, the projection method introduced by Morbiducci [20], Arzani and Shaden [21] and implemented in COMSOL® by Richter et. al [14], is applied. For that, the centerline vectors \vec{c} , connecting the subsequent centerline points, are projected to the artery surface. The projection process is split up into two parts. First, for every point on the surface a search algorithm is executed, which searches for nearest centerline points within a specific distance. If no point is found the search distance ascends. But only those centerline points, whose connection vector to the considered surface point has the same orientation as the outer normal vector to this surface point are considered. This is of special importance in sites of artery branching and guarantees the selection of centerline points corresponding to the currently considered branch surface. From the collected points the centerline point, whose connecting vector is most perpendicular to the centerline vector \vec{c} , is finally chosen. After applying this searching algorithm for each point on the surface, the final list of surface point coordinates and

the corresponding centerline vectors \vec{c} are saved in one TXT document and imported to our COMSOL® simulation template.

The second step is achieved in the COMSOL® interface itself. Here the chosen centerline vectors \vec{c} , moved to the corresponding artery surface points (mesh nodes), are projected into the artery surface planes by the formula

$$\mathbf{t}_\ell^i = \frac{\vec{c}^i - (\vec{c}^i \cdot \mathbf{n}^i)\mathbf{n}^i}{\|\vec{c}^i - (\vec{c}^i \cdot \mathbf{n}^i)\mathbf{n}^i\|}, \quad (14)$$

to obtain centerline (longitudinally) aligned surface tangent vectors, for each surface node. Here \mathbf{n}^i is the outside normal vector of the i -th surface node. The tangential vectors constructed in this way are presented in Fig.8.

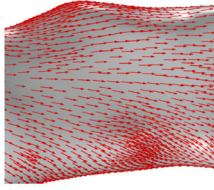


Figure 8: Constructed centerline-aligned tangent field \mathbf{t}_ℓ , [14].

The outcomes of the preprocessing are three TXT files, that are serving as basis for the individual simulation. A parameter list ‘patient_xy_Parameterliste.txt’, where the center points and normal vectors for the outlet perimeter cut planes and parameters for the evaluation slicing planes are saved. A variable list ‘patient_xy_Variablenliste.txt’ contains the expressions for the resistance boundary conditions and for the geometric filters. And finally, the file ‘patient_xy_tangentialField.txt’ provides the longitudinal tangential surface vector field for the evaluation of longitudinal WSS.

Simulation template

To set up each of the 110 patient simulations, similar adjustments must be made for all simulations. To streamline these tedious and time-consuming steps, we have developed a simulation template in COMSOL® that contains prepared nodes and settings needed for all simulations.

This includes all characteristic features of the simulation, such as the laminar flow physics with the wall (non-slip) boundary condition at the artery surface, the pulsating flow profile at the inlet, the definition of integration operators applied at the inlet and outlets to calculate the flowrates for the resistance boundary conditions (7), the definition of geometrical units as inlet, outlets, wall, (with the Selection operator, cp. Fig. 2), the definition of variables used to store the constructed longitudinal tangential vectors (14), etc. To achieve an automated simulation setup, we use a referencing

Name	Expression	Value	Description
Int_Ex1	-18.6436	-18.644	
Int_Ey1	19.9463	19.946	
Int_Ez1	-56.2877	-56.288	
Int_Ex2	0	0	
Int_Ey2	0	0	
Int_Ez2	-678.5943	-678.59	
Int_Ex3	1	1	
Int_Ey3	0	0	
Int_Ez3	-708.6812	-708.68	
Bif_Ex1	-17.414	-17.414	
Bif_Ey1	18.1036	18.104	

Figure 9: Table of imported simulation parameters obtained in geometric preprocessing.

system that refers to a set of general names for parameters, variables, operators, and geometric selections that are prepared morphology-specific in preprocessing. In Fig. 2 the use of precomputed variables and predefined integral operators over specific geometric selections (framed in red) is illustrated in the implementation of resistance boundary condition.

With our COMSOL® template in hand, the following steps complete the simulation preparation for an individual CA geometry in COMSOL®. Each component of the tangential field $\mathbf{t}_\ell = (t_x, t_y, t_z)$ is loaded as variable into a designated function node. Since the template is prepared for up to 7 artery branches, all unused nodes and operators must be disabled in case of CA-tree with less branches before starting the simulation. Then the geometry mesh must be imported from the STL file into the mesh node, whereby edge and surface fragments, byproducts of previous geometry processing steps, are deleted, if necessary. After importing the cleaned-up mesh into the geometry node, geometry cropping is performed to define the inlet and outlet cross sections. This is done using perimeter planes, see Fig. 10, derived from cylindrical objects rather than using the working planes available in COMSOL®. Note, that the latter have an infinite range and can trim the geometry in more than just the desired location, while the perimeter planes can be designed appropriately to trim only one branch. To prevent unnecessary cuttings of the geometry is important for the workflow, which may be permanent and irreversible, and may lead to an ‘internal geometry decomposition error’ during the geometry building. The center

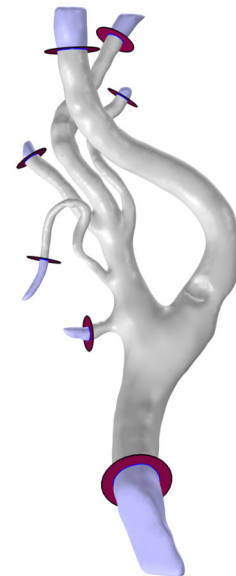


Figure 10: Perimeter planes for geometry cropping.

points and normal vectors, determined in geometric preprocessing from the centerline are used for the construction of the bases of cylinders. COMSOL® geometry utility Convert to Surface is applied to the cylinder volume objects, the resulting surfaces, except for the base of the cylinder, are deleted to obtain the desired perimeter planes. For the deletion of objects (cylindric surfaces or cut off artery ends) manual choice by clicking on the objects is necessary during the geometry construction steps. Af-

ter completing the geometry cutting, the Selection operators must be assigned manually to the corresponding geometric entities as the vessel wall, inlet and outlet surfaces to put the geometry referencing system into effect. Finally, COMSOL® intern mesh

generator needs to be executed. In our simulation template, *physic-based* mesh with *finer* mesh quality is chosen, resulting in mesh with refined boundary layers and various numbers of mesh elements along all 110 cases, depending on the complexity of the artery morphology, see Fig.12. The fluid-flow time-

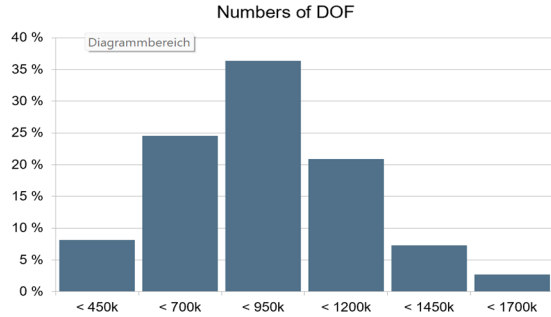


Figure 12: Distribution of degrees of freedom (DOF) over the 110 simulations, mean DOF~833k.

dependent study is set up over two complete cardiac cycles with the built-in PARDISO solver and the adaptive time-stepping BDF algorithm using P1+P1 finite elements.

After importing the preprocessed parameters and data, and after all described manipulations and assignments, the template is ready for simulation. To streamline the simulation process, simulations are prepared for a larger batch of arteries in one go and started automatically from queue.

Postprocessing and data export

After completing the numerical simulations, numerical data are exported within the *result node* of our COMSOL®-template. Here volume fields as well as scalar quantities such as velocity, pressure or vorticity

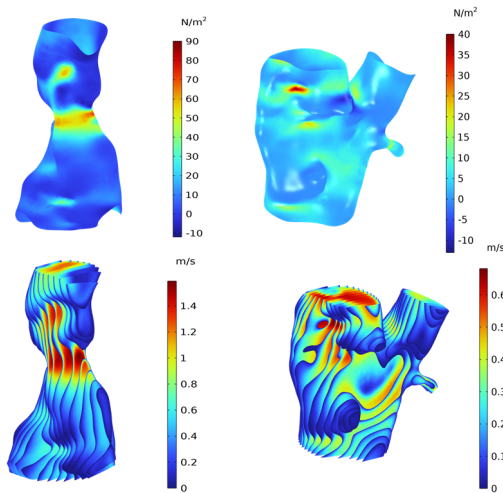


Figure 11: Examples of exported surface (WSS) and volume field (velocity) data.

are saved in a VTU file format. The stroke risk descriptors WSS and OSI are evaluated on the artery surface. At this point, the geometric filters for the bifurcation and initial interna branch are applied to the export data. Since the evaluation of both OSI indicators (10), (11) requires the integration of the corresponding wall shear stresses over time, i.e., the

global evaluation, this step is the most time-consuming part of the post processing. Finally, all surface and slice data are saved pointwise in a TXT file format with specific name patterns to simplify their further usage.

Conclusion: Hemodynamic Database Creation

The above-described workflow has been applied to artery geometries in 10-20 artery batch steps. For the whole batch of individual cases first the out-of-COMSOL geometric preprocessing steps were performed. Then the simulation templates have been adjusted for individual case by importing the corresponding files of parameters and variables as well as longitudinal tangent vectors. Simulations have been started from the queue with help of a short shell script. The computations have been done on Intel(R) Xeon(R) Gold 5122 CPU at 3.60 GHz with 4 cores, where the average computational time was 4 h 50 min. The average time costs for one individual patient artery including the fluid flow simulation and evaluation risk indicators derived from numerical solution, broken down by the preprocessing, the individual manipulations/corrections, the simulation itself and the postprocessing are presented in Table (1).

Preprocessing	30 min
Individual correction	10 min
Mean computation time	4 h 50 min
Postprocessing	2 h
Total	7 h 30 min
Overall time for 110 geometries	34 d 9 h

Table 1: Time costs for every step of the workflow.

Finally, the postprocessed data form a hemodynamic database with different data types that can be extended with new patient cases utilizing our automated simulation workflow. These already existing database has been used to successfully train a neural network which can categorize different stenosis degrees depending on the WSS. Furthermore, these simulations were the groundwork for an explorative visualization tool of the carotid morphology specifically designed for practicing physicians.

Acknowledgements

This work was funded by the German Federal Ministry of Education and Research (BMBF) joint project MLgSA, Subproject 05M20UNA

References

- "
- [1] WHO, "The top 10 cause of death," December 2019. [Online]. Available: <https://www.who.int/news-room/fact-sheets/detail/the-top-10-causes-of-death>. [Accessed September 2023].

- [2] "Centers of Disease Control and Prevention," 2023. [Online]. Available: <https://www.cdc.gov/heartdisease/facts.htm>. [Accessed September 2023].
- [3] E. Debus, G. Torsello, G. Schmitz-Rixen, I. Flessenkämper, M. Storck, W. H. and R. Grundmann, "Ursachen und Risikofaktoren der Arteriosklerose," *Gefäßchirurgie*, vol. 18, pp. 2413-2419, 2013.
- [4] A. Iannuzzi, P. Rubba, M. Gentile, V. Mallardo, I. Calcaterra, A. Bresciani, G. Covetti, G. Cuomo, P. Merone, A. Di Lorenzo, R. Alfieri, E. Aliberti, F. Giallarua, M. Di Minni and G. Iannuzzo, "Carotid Atherosclerosis, Ultrasound and Lipoproteins," *Biomedicines*, vol. 9, no. 5, 2021.
- [5] J. L. M. Björkegren and J. L. Aldons, "Atherosclerosis: Recent developments," *Cell*, vol. 185, pp. 1630-1645, 2022.
- [6] P. Libby, "The changing landscape of atherosclerosis," *Nature*, vol. 592, pp. 524-533, 2021.
- [7] P. Eulzer and K. Lawonn, "A Dataset of Reconstructed Carotid Bifurcation Lumen and Plaque Models with Centerline Tree," 2023. [Online]. Available: <https://zenodo.org/record/7634644>.
- [8] L. Zarrinkoob, K. Ambarki, A. Wahlin, R. Birgander, A. Eklund and J. Malm, "Blood flow distribution in cerebral arteries," *Journal of Cerebral Blood Flow & Metabolism*, vol. 35, pp. 648-654, 2015.
- [9] R. S. Seymour, Q. Hu and E. P. Snelling, "Blood flow rate and wall shear stress in seven major," *J. Anat.*, vol. 236, pp. 522-530, 2020.
- [10] I. E. Vignon-Clementel, C. A. Figueroa, K. E. Jansen and C. A. Taylor, "Outflow boundary conditions for three-dimensional finite element modeling of blood flow and pressure in arteries," *Comput Methods Appl Mech Eng.*, vol. 195, no. (29-32), p. 3776-3796, 2006.
- [11] C. Taylor, T. J. R. Hughes and C. Zarins, "Finite element modeling of three-dimensional pulsatile flow in the abdominal aorta: relevance to atherosclerosis," *Annals of Biomedical Engineering*, vol. 26, pp. 975-987, 1998.
- [12] D. Ku, D. Giddens, C. Zarens and S. Glagov, "Pulsatile flow and atherosclerosis in the carotid bifurcation, positive correlation between plaque location and low oscillating shear stress," *Arteriosclerosis*, vol. 5, pp. 293-302, 1985.
- [13] A. Hoogendoorn, E. M. Hartman, A. Kok and G. De Nisco, "Multidirectional wall shear stress promotes advanced coronary plaque development - comparing five shear stress metrics," *Cardiovascular Research*, vol. 116, no. 6, pp. 1136-1146, 2019.
- [14] K. Richter, T. Probst, A. Hundertmark, E. Pepe and K. Lawonn, "Longitudinal wall shear stress evaluation using centerline projection approach in the numerical simulations of the patient-based carotid artery," *Computer Methods in Biomechanics and Biomedical Engineering*, 2023.
- [15] V. Pfeiffer, S. J. Sherwin and P. D. Weinberg, "Does low and oscillatory wall shear stress correlate spatially with early atherosclerosis? A systematic review," *Cardiovascular Research*, vol. 99, no. 2, pp. 242-250, 2013.
- [16] C. K. Zarins, D. P. Giddens, B. K. Bharadvaj, V. S. Sottirai, R. F. Mabon and S. Glagov, "Carotid bifurcation atherosclerosis. Quantitative correlation of plaque localization with flow velocity profiles and wall shear stress," *Circulation Research*, vol. 53, pp. 502-514, 1983.
- [17] M. Blagojevic, A. Nicolice, M. Zivkovic, G. Stankovic and A. Pavlovic, "Role of oscillatory shear index in predicting the occurrence and development of plaque," *Journal of the Serbian Society of Computational Mechanics*, vol. 7, no. 2, pp. 29-37, 2013.
- [18] J. W. Eaton, D. Bateman, S. Hauberg and R. Wehbring, "GNU Octave version 8.2.0 manual: a high-level interactive language for," [Online]. Available: <https://www.gnu.org/software/octave/doc/v8.2.0/>
- [19] B. D. Team, "Blender," 2023. [Online].
- [20] U. Morbiducci, D. Gallo, S. Cristofanelli, R. Ponzini, M. A. Deriu, G. Rizza and D. A. Steinmann, "A rational approach to defining principal axes of multidirectional wall shear stress in realistic vascular geometries, with application to the study of the influence of helical flow on wall shear stress directionality in aorta," *Journal of Biomechanics*, vol. 48, no. 6, pp. 899-906, 2015.
- [21] A. Arzani and S. S. C., "Characterizations and correlations of wall shear stress in aneurysmal flow," *Journal of Biomechanical Engineering*, 2015.
- [22] L. Antiga, *Patient-specific Modeling of Geometry and Blood Flow in Large Arteries*, Milan: Politecnico di Milano, 2002.
- [23] K. Perktold and G. Rappitsch, "Computed Simulation of local blood flow and vessel mechanics in a compliant carotid artery bifurcation model," *Journal of Biomechanics*, vol. 28, no. 7, pp. 845-856, 1995.